

BASIC FEATURES OF THE PREDICTIVE TOOLS OF EARLY WARNING SYSTEMS FOR WATER-RELATED NATURAL HAZARDS: EXAMPLES FOR SHALLOW LANDSLIDES

Roberto Greco

Associate Professor

University of Campania Luigi Vanvitelli, Italy

roberto.greco@unicampania.it

Luca Pagano

Associate Professor

University of Naples Federico II, Italy

luca.pagano@unina.it

ABSTRACT

To manage natural risks, an increasing effort is being put in the development of early warning systems, which rely on prompt forecasting or recognizing of the catastrophic phenomena and temporarily reducing the exposure of people, preventing or limiting victims. Research efforts aimed at the development and implementation of effective EWS should concern, above all, the definition and calibration of the interpretative model. This paper analyses the main features characterizing predictive models working in early warning systems, by discussing their aims, the evolution stage of the phenomenon where they should be incardinated, and their architecture, regardless of the specific application field. With reference to ~~two different phenomena, namely~~ flow-like landslide and earth flows, both characterized by rapid evolution, the paper describes, by means of three examples, some ~~alternative~~ approaches to the development of the predictive tool and to its implementation in an EWS.

1. INTRODUCTION

Different natural phenomena turning into catastrophes have occurred widespread in Italy in the recent past as well as in the last centuries. Seismic and volcanic phenomena have affected sporadically large areas, while rainfall-induced landslides, floods and snow avalanches have frequently hit sites spread all over the territory. Structural mitigation approaches are inapplicable throughout the entire territory at risk and might be planned only for areas relevant from a socio-economic point of view.

Hence, to manage natural risks, an increasing effort is being put in the development of non-structural approaches, which rely on prompt forecasting or recognizing of the catastrophic phenomena, so to early spread the alarm throughout the exposed areas (early warning) and temporarily eliminate or, at least, reduce the exposure of people, preventing or limiting victims.

Early Warning Systems (EWS) are among the priorities adopted by the United Nations, International Strategy for Disaster Reduction (ISDR) (UN-ISDR, 2005). They indeed present undeniable advantages, among which are their fast, simple and low-cost implementation, and environmental friendliness. Focusing on water-related hazards, significant examples of operational early warning systems are currently found in the field of floods, landslides, snow avalanches, earth fill failures. A recent review of EWS operating in Europe for water-related hazards can be found in Alfieri et al. (2012).

As it will be described in detail hereinafter, the architecture of an EWS is strictly related to the time needed for the deployment of the mitigation measures, compared to the time of evolution of the hazardous event. In this respect, EWS for floods present quite different features if they are established along large or small rivers. ~~In the first case, rainfall measurements or predictions are supplemented with river stage measurements in upstream sections (e.g. Rabuffetti and Barbero, 2005), and flood routing models can be run in cascade of hydrological models (e.g. Cranston and Tavendale, 2012). The lead time of prediction, which depends on the length of the river and on the extension of its catchment, can extend up to several days or weeks.~~ In the case of small streams, the time lapse between rainfall and peak discharge may be so short that weather now castings needed for the warning to be launched in due time (e.g. Alfieri and Thielen, 2015; de Saint-Aubin et al., 2016).

So far, most of the EWS dealing with rainfall-induced landslides are based on rainfall measurements, sometimes supported by weather forecasts (e.g. Keefer et al., 1987; Ponziani et al., 2012), rarely integrated with monitoring of some soil variables (e.g. Ortigao and Justi, 2004; Chleborad et al., 2008; Baum and Godt, 2010). Rainfalls are

1 interpreted often merely statistically, with an empirical quantification of rainfall
2 thresholds for landslide initiation (e.g. Guzzetti et al., 2007, 2008; Tiranti and
3 Rabuffetti, 2010, Sirangelo and Versace, 1996; Sirangelo and Braca, 2004). In rare
4 cases, physically based approaches are adopted for the interpretation of the effects
5 of rainfall history. The few examples of inclusion of slope infiltration and stability
6 modelling in the assessment of the safety conditions are mostly still at a prototypal
7 stage (e.g. Schmidt et al., 2008; Ponziani et al., 2012; Eichenberger et al., 2013; Pumo
8 et al., 2016).

~~9 EWS operating for snow avalanches monitor snow accumulation and the melting
10 processes, with the former basing essentially on interpreting precipitation and air
11 temperature records, and the latter on air (or snow) temperature (e.g. Liu et al.,
12 2009).~~

~~13 Even in the field of man-made systems, early warning is assuming a prominent role in
14 the assessment of the risk associated with failure. For instance, in the field of earth
15 dams, with regard to all possible collapse mechanisms, i.e. slope instability and
16 internal erosion phenomena, or even earthquake-induced effects, risk mitigation is
17 de-facto based on early warning systems (e.g., Pagano & Sica, 2013; Ma and Chi,
18 2016). The wide monitoring system commonly installed to characterize time-by-time
19 the behavior of these structures, carried out essentially in terms of displacements,
20 pore water pressure, seepage flows, accelerations, is pointed towards a continuous
21 checking of dam safety conditions, aimed at evacuating downstream settlements in
22 case of predicted collapse.~~

~~23 In the different fields above considered, literature indicates that common elements,
24 which typically characterize an early warning system, are:~~

- ~~25 1. *a field monitoring system*, recording physical quantities related to the
26 phenomenon in hand, and transmitting them to a collection-elaboration center;
27 measured variables may conveniently be distinguished into two categories: *cause*
28 *variables*, leading to the initiation of the phenomenon; *effect variables* that,
29 affected by the formers, characterize the phenomenon itself at the triggering
30 stage or during its evolution, allowing also to recognize its intensity;~~
- ~~31 2. *an interpretative model*, formalizing mathematically the relationships linking
32 cause and effect variables, allowing to catch the evolution stage of the
33 phenomenon and assess system safety conditions;~~
- ~~34 3. *thresholds* for the variables related to safety conditions of the system; these
35 thresholds correspond to different alert levels, with the highest one activating the
36 spread of the alarm message, aimed at eliminating people exposure;~~

4. different *actions* related to each alert level defined at 3.

Research efforts aimed at the development and implementation of effective EWS should concern, above all, the definition and calibration of the interpretative model (Michoud et al., 2013). It should be as accurate as possible and, at the same time, capable of rapidly carrying out the turning of the monitored quantities into the assessment of system safety conditions. In many applications, dealing with rapidly evolving **phenomena**, a real-time working system is in fact required, in order to maximize the lead time available for people exposure elimination.

This paper analyses the main features characterizing predictive models working in early warning systems, by discussing their aims, the evolution stage of the phenomenon where they should be incardinated, and their architecture, regardless of the specific application field. Then, examples of application to EWS for rainfall-induced landslides are presented. ~~In particular, the proposed examples refer to the case of cohesionless shallow covers, chosen~~ as they pose challenges that are quite representative of a number of other natural phenomena that might be mitigated by means of early warning systems.

2. PREDICTION UNCERTAINTY AND THE MINIMIZATION OF THE COSTS OF MISSING AND FALSE ALARMS OF AN EWS

Whatever the predictive model adopted, it will never be capable of providing certainty about the occurrence of a **destructive phenomenon**. ~~A model yields variables systematically affected by a given uncertainty degree due to the following possible causes:~~

- ~~- incompleteness of information about the physical system supposed to cause catastrophes;~~
- ~~- various error types associated with the measurements provided by the monitoring system;~~
- ~~- unavoidable simplifications of reality introduced in the predictive model;~~
- ~~- randomness of some of the processes involved in the genesis of the catastrophic event.~~

~~It is obvious that all the uncertainties of the predicted variables related to the physical system safety affect the assumption of different alert stages. With reference to the last stage, it~~ may occur that the early warning system sends an alarm, but no dangerous phenomena occur (false alarm) or, conversely, that a dangerous phenomenon takes place without any issued alarm (missing alarm). Both false and

1 missing alarms result into costs for the community supplied with the EWS. A lower
2 uncertainty degree in the prediction is required to minimize their number and,
3 consequently, costs during the system operation. Efficiency of the EWS is therefore
4 considered with respect to the system economic performance for the community,
5 rather than to safety performance. In this sense, alarm activation has to account for
6 the uncertainties associated with each alert threshold and its overcoming, so to
7 minimize false and missing alarms and related costs.

8 Decisional rules regarding actions associated with each alert threshold should be
9 based not only on the mere quantification of thresholds themselves, but also on
10 criteria defining the *sensitivity* of the EWS, intended as setting the activation of the
11 system at some probability of a given threshold to be exceeded.

12 The most suitable strategy to quantify such probability of threshold exceedance
13 cannot be generalized. It is in fact strongly affected by the following peculiarities
14 characterizing the EWS in hand:

- 15 - the uncertainty of the prediction, which may be reduced by increasing the initial
16 investment (by preliminary acquiring more information about physical system
17 features, implementing a more reliable monitoring system with higher spatial and
18 temporal resolution, elaborating a more sophisticated and accurate predictive
19 model);
- 20 - the costs suffered by the community in case of false alarm, in turn depending also
21 on the kind of actions planned in case of threshold exceedance;
- 22 - the costs resulting from a missing alarm with catastrophic event occurrence,
23 depending on both the event (type and intensity) and resilience of the exposed
24 goods (related to their nature as well as to socio-economic aspects).

25 In setting up the sensitivity of the EWS, it should be taken into account that too many
26 false alarms would discredit the system, implying that, with the passing of time, the
27 served community would contribute less in carrying out all the required actions after
28 alerts. In short, the sensitivity has to be calibrated on the basis of a cost-benefit
29 analysis, which can be properly carried out only if the uncertainty of model
30 predictions can be estimated after an adequate period of monitoring of the physical
31 system.

3. EVOLUTION STAGES OF A NATURAL HAZARD: WHEN SHOULD THE MODEL DO THE PREDICTION?

In order to generalize a typical architecture for the predictive model, it comes useful to account for a conventional sequence of stages describing the evolution of a natural phenomenon resulting into a catastrophe (Figure 1):

- (a) the predisposing stage: the **cause** variables are subject to such changes to induce significant modifications of effect variables; the EWS crosses the intermediate alert thresholds, **approaching the alarm threshold**;
- (b) the triggering and propagation stage: the failure occurs locally (triggering time) and propagates from point to point throughout the physical system up to get the physical system itself entirely involved;
- (c) the paroxysmal stage: the physical system collapses and the kinematic of the system goes on, eventually hitting the exposed goods.

The duration of each stage may greatly vary, depending on both the **phenomenon** type and on the features of the physical system involved.

~~In a seismic phenomenon involving structures located at a given site "S", the *predisposing stage* (a) is determined by the occurrence of the seismic event at the epicenter and is indicated by the first arrival of the seismic waves at the seismometers nearest to the epicenter. The *triggering and propagation stage* (b) is determined by acceleration values exceeding the threshold for first local damages to structural elements and is monitored by seismic stations located at "S"; the *paroxysmal stage* (c) consists of the collapse of parts of the structures. For this specific example, the duration of the stages (a) and (b) is few tens of seconds, while the duration of the stage (c) depends on the system considered, spanning from seconds for systems like buildings, rock slopes, gas conduits etc., until hours or even days for natural earth slopes, dams, and, in general, systems which collapse is determined by a slow redistribution or propagation of earthquake induced effects.~~

In a rainfall-induced landslide, the *predisposing stage* (a) is determined by the sequence of rainfall events increasing pore water pressure and worsening slope stability conditions. The *triggering and propagation stage* (b) spans from the first local slope failure until the formation of a slip surface. The *paroxysmal stage* (c) is the sliding of the mobilized soil mass downhill along the slip surface. In this ~~second~~ example, the duration of each stage is strongly related to the geomorphology of the specific slope, and may vary from minutes (e.g., flow slides in slopes covered with

1 shallow coarse grained soils) to even years (e.g., earth flows in slopes of fine grained
2 soils).

3 ~~In a snow-avalanche, the *predisposing stage* (a) is determined by snow accumulation~~
4 ~~and temperature increments; the *triggering and propagation stage* (b) starts when~~
5 ~~local failures take place within the snow aggregate and ends with a slip surface~~
6 ~~formation. The *paroxysmal stage* (c) starts when the mass slides downhill. In this~~
7 ~~example, the duration of stage (a) may be of hours or days, depending on the~~
8 ~~evolution of atmospheric variables, the duration of stage (b) results undetectable, and~~
9 ~~the paroxysmal stage lasts only few seconds.~~

10 For the case of an overflow in a river, the *predisposing stage* (a) is a sequence of
11 precipitation events within the watershed, causing a progressive increase of the water
12 level along a branch of the river; in this case, the *triggering and propagation stage* (b)
13 and the *paroxysmal stage* (c) are hardly distinguishable from each other. In fact, both
14 stages start when the first local overflow takes place, and both develop with the flood
15 propagating around the river. The stage duration depends on the extension and
16 geomorphology of the watershed. The entire phenomenon may last tens of minutes
17 (e.g., flash floods in small streams with relatively small catchment) to several days
18 (e.g., large rivers with large hydrographic basin).

19 It is also important to highlight that **for most phenomena** the triggering event has to
20 be considered as random and, as such, time and location of its occurrence can be
21 predicted only with a probabilistic approach. On the other hand, the predisposing
22 stage can be usually described with physical laws, so that its spatial and temporal
23 evolution can be predicted deterministically by mathematical models.

24 ~~For instance, the strategies followed for early warning with respect to snow~~
25 ~~avalanches (e.g., Bakkeoi, 1987) neglect the detection of any possible triggering~~
26 ~~cause. These may be internal to the physical system (related to some peculiar~~
27 ~~morphologies favoring the susceptibility to local failures) or external (e.g., a skier path~~
28 ~~cutting transversally the snow layer slope or a rock-mass falling onto the layer). The~~
29 ~~randomness of such kind of triggering causes make them undetectable and useless~~
30 ~~for early warning purposes. However, it should be noted that these causes may~~
31 ~~become effective only if a predisposing state takes place in terms of snow layer~~
32 ~~thickness and temperature. This leads to define the different alert levels on the basis~~
33 ~~of these two factors, for which experimental quantification is easy and reliable.~~
34 ~~Consequently, the warning does not deal with exactly identifying when, where and~~
35 ~~what specific triggering cause might generate an avalanche.~~

1 In general, early warning prediction can be carried out during any of the above-
2 defined evolution stages. The choice of the particular stage should obviously consider
3 that elapsed times needed to predict the event, spread the alarm and eliminate
4 people exposure must not exceed the time after which the destructive event occurs.
5 On the other side, the limited time available in-between prediction and event should
6 indicate which kind of actions could be reasonably carried out. So, only in some cases
7 it will be possible to consider the opportunity to evacuate all buildings of an entire
8 neighborhood or forbid all exposed streets to traffic and people access. In some cases,
9 the small available time only leaves the opportunity for some short actions, such as
10 the interruption of dangerous supplied services (gas and electricity) or closure of
11 important infrastructures highly exposed, such as railways or highways.

12 The first step that has to be followed in the development of the predictive tool is
13 hence the detailed study of the mechanisms that control the evolution of the
14 phenomenon in hand, and identify which phenomenon stage is the most suitable for
15 the assessment of safety conditions. For some problems, the choice necessarily falls
16 into a specific stage, while for others the choice may be multiple. For instance, the
17 slow kinematic of landslides in fine grained soils allows to place the predictive tool in
18 any of the above defined three stages, while the rapid kinematic of rainfall-induced
19 landslides in coarse grained soils prevents considering the paroxysmal stage.

20

21 **4. THE ARCHITECTURE OF THE PREDICTIVE MODEL**

22 The second step of the development of the predictive tool is choosing the
23 interpretative model. Promptness and reliability are mandatory requirements of the
24 prediction. The promptness is usually obtained by introducing model simplifications,
25 which should however not imply excessive accuracy losses, because they would
26 increase uncertainties and, consequently, false and missing alarms. An increase of
27 model complexity should correspond to a reduction in the observational scale of the
28 phenomenon. Complex models can only be applied to slope scale problems, while,
29 increasing the observational scale from local to regional, progressive simplifications
30 have to be introduced in the model and, consistently, less ambitious goals have to be
31 set in terms of reliability.

32 The wide variety of applications for EWS makes it difficult to generalize criteria to
33 guide the choice of the predictive model. It is only possible to refer to some
34 classification criteria, of aid in clarifying the philosophy of the chosen approach, and
35 what ingredients it requires for its best implementation.

1 A first classification criterion distinguish between empirical and physically-based
2 models. Empirical models extract relationships among cause and effect variables from
3 available monitoring data taken over a prolonged time interval. Once set up the
4 empirical relationships, they typically do not take into any account the physics
5 governing the phenomenon. Their reliability essentially depends on the amount,
6 accuracy and representativeness of the available data-set.

7 On the other hand, physically-based models relate cause and effect variables through
8 mathematical relationships derived straightforwardly from the physical principles
9 governing the considered phenomenon. The mathematical description of the model
10 typically involves the assumption of simplifications that strongly affect the accuracy
11 of the prediction.

12 These two categories may also be used contextually in setting up predictive tools
13 consisting of physically-based as well as of empirical steps.

14 The second criterion of classification refers essentially to physically-based models,
15 and is strictly related to the need for a rapid prediction. It distinguishes between on-
16 line and out-of-line predictions. The former consist in real-time solution of the model
17 equations, updated continuously over time with changes in boundary conditions
18 indicated by field monitoring. The latter, instead, define simple mathematical
19 equations or abaci relating cause and effect variables, by solving the governing
20 equations preliminarily for a number of possible scenarios in terms of initial and
21 boundary conditions (e.g, Pagano & Sica, 2013). These simple mathematical equations
22 or abaci represent the predictive tools adopted to rapidly interpret the data from field
23 monitoring.

24 Strictly related with the selection of the model is, finally, the design of the monitoring
25 system. It has to be consistent with all the choices made about the previously
26 illustrated points. The considered specific stage of phenomenon evolution, as well as
27 the choice of the predictive model, unequivocally identify the physical variables to be
28 monitored, their location and, finally, the number of measurement points.

29 In the following sections, the different features above highlighted will guide along the
30 illustration of some application cases developed in the field of rainfall-induced flow-
31 like landslides.

32 33 **5. EXAMPLES OF SET UP AND CALIBRATION OF THE PREDICTIVE TOOL FOR EARLY** 34 **WARNING**

1 In Italy the destructive potential of rainfall-induced rapid flowslides and debris flows
2 is sadly known. The significance of the problem in terms of number of events and
3 victims becomes clear by merely referring to the disasters occurred over the last years
4 in Campania (Cascini&Ferlisi, 2003, Calcaterra et al., 2004; Pagano et al., 2010; Santo
5 et al., 2012), Piedmont (Villar Pellice, occurred in 2008), Liguria (Cinque Terre,
6 occurred in 2011) and Sicily (Maugeri et al., 2011). The rapid kinematic characterizing
7 the post-failure behavior of these phenomena implies that the setup of an early
8 warning system may not rely on the analysis of the short-lasting paroxysmal stage
9 (Figure 2).

10 Exception is made for early warning systems implemented along some roads or
11 railways where the probability that the sliding mass detaching from a slope directly
12 impacts vehicles is small, while the probability that vehicles crash against previously
13 fallen mass obstructing the road is much higher. In such cases, the alarm might be
14 launched in case of the feared road invaded by fallen masses. Hence, the alarm itself
15 could be based on promptly gathering the occurrence of slope instabilities by carrying
16 out monitoring of displacements, and inhibiting road access in case of recorded
17 movements exceeding some threshold (Mannara et al., 2009).

18 If the exposed factor is instead likely to be directly impacted by the sliding mass, the
19 triggering of the instability must be predicted in due advance. The time span required
20 to eliminate people exposure, typically some hours ~~long~~, implies that the prediction
21 should be based on monitoring and interpretation of triggering precursors, carried
22 out already during the predisposing stage.

23 The phenomena in hand typically involve the mobilization of shallow covers rarely
24 exceeding 2 meters in thickness, induced by rainfall infiltration and related suction
25 drop. Further physical variables governing the phenomenon are effect variables
26 describing soil cover wetting (degree of saturation, water content, water storage).

27 The predictive tool may be built on empirical bases whereas, for the reference
28 geographical context, historical ~~monitoring data of rainfalls~~ related to their effects are
29 available. Alternatively, it is possible to adopt physically-based approaches through
30 which turning at any time rainfall into effect variables related to slope stability
31 conditions. Different levels of these effect variables or, alternatively, of slope stability
32 indices derived from them, may be chosen as the alert thresholds of the early warning
33 system. If the mathematical model of the slope has been properly simplified, it may
34 be possible to operate "in line" by performing model simulations in few minutes.

35 Recent advances in field monitoring of effect variables, in particular soil suction
36 and/or water content, nowadays offer an alternative approach to the interpretation

of rainfall effects. Sensors like tensiometers, heat dissipation probes and TDR probes, in principle could directly deliver all the effect variables needed for the assessment of slope stability conditions. However, the spatial variability of soil properties likely makes an EWS relying only on field monitoring of effect variables unreliable. Field data are in fact always affected by local issues, and so they are poorly representative of the whole monitored area, unless an extremely rich network of sensors is installed, which in most cases is unfeasible. Hence, field monitoring should be deployed supplementing, rather than replacing, the estimation of effect variables by means of a more or less simplified estimation of rainfall effects.

The following application examples refer to single slopes, with extension of few hectares, located in the Lattari Mountains (Campania, southern Italy) and in the basin of Stura di Lanzo (Piedmont, northern Italy).

Empirical approach based on rainfall records

The example herein reported refers to the chain of Lattari Mountains and, in particular, to an area spreading in-between the towns of Pagani and Nocera Inferiore (Campania, southern Italy). An intensely fractured calcareous bedrock covered by silty volcanic soils characterizes the geology of the site. Volcanic covers have formed due to pyroclastic air-fall deposits generated by eruptions, mainly those of the volcanic complex of Somma-Vesuvius occurred over the last 40000 years. Several rainfall-induced flow-like landslides have interested these covers over centuries. Numerous phenomena also occurred in the recent past, usually triggered along slopes with inclination angle between 30° and 40°.

A pluviometer installed in 1950, around 3 Km far from the downslope area, provides a daily rainfall series spanning over 50 years (Pagano et al., 2010). During this period, three significant flow-like landslides occurred in 1960, 1972 and 1997. Daily rainfall heights triggering the three phenomena were 87, 77 and 110 mm, respectively. Figure 3 shows all the observed daily rainfall heights larger than the minimum value followed by a landslide ($h_{dL} = 77\text{mm}$), plotted in ascending order. It may be noticed that the condition $h_{dS} > h_{dL}$ was met 39 times, but only twice a landslide was actually triggered. This low correspondence between daily rainfalls and landslides depends on the existence of additional influencing factors, related to the conditions of the soil cover at the onset of triggering rainfall, which are neglected if only daily rainfall height is considered. Antecedent precipitation, in particular, is supposed to play a crucial role, as it determines the amount of water stored in the cover and lowering soil suction significantly, before the crucial suction drop induced by the triggering rainfall.

1 The effects of antecedent precipitations may be taken into account by assuming that,
2 besides the rainfall directly triggering the event (usually identified with rainfall fallen
3 during the last day), also ~~rainfall cumulating over a longer antecedent period (h_x)~~ plays
4 an important role in establishing the predisposing conditions for the triggering of a
5 landslide. The duration “x” of the antecedent period may be chosen as the one
6 minimizing the number of events (h_{ds} , h_x) characterized by h_x similar to the antecedent
7 precipitation, h_{xL} , accumulated before the three observed landslides. The
8 minimization yielded $x=2$ months. This ~~value for x~~ corresponds to h_{2mL} values for all
9 three landslides of about 500 mm. Over the reference period only 5 rainfall histories
10 (h_{ds} , h_{2m}) resulted similar to the three (h_{dL} , h_{2mL}) which were followed by in a landslide.
11 If this double threshold criterion had been virtually implemented as early warning
12 criterion in the considered area, it would have produced 5 false alarms over 50 years.

13

14 **Stochastic approach**

15 Few examples of real-time predictions of the probability of triggering of rainfall-
16 induced landslides in a small area (i.e. a slope or a small catchment) can be found in
17 the literature (e.g. Sirangelo and Versace, 1996; Sirangelo and Braca, 2004; Schmidt
18 et al., 2008; Greco et al., 2013; Capparelli et al., 2013; Manconi and Giordan, 2016;
19 Ozturk et al., 2016). This is due to the intrinsic difficulty of having available historical
20 data sets of rain storms and corresponding landslides occurred in a small area, with
21 enough data to allow reliable estimation of the probability of landslide triggering
22 during extreme (and thus rare) rainfall events. Usually, only few landslides occur at a
23 site during an observation period of typically some decades, so that probabilistic
24 landslide initiation thresholds are mostly defined at regional scale, so to have a rich
25 data set of observed landslides (e.g. Terlien, 1998; Guzzetti et al., 2007; 2008; Jakob
26 et al., 2012; Ponziani et al., 2012; Segoni et al., 2015; Iadanza et al., 2016). The use of
27 physically based models of infiltration and slope stability can help in the prediction of
28 slope response under conditions different from those actually encountered during the
29 observation period, thus allowing the definition of site-specific landslide initiation
30 thresholds (e.g. Arnone et al., 2011; Ruiz-Villanueva et al., 2011; Tarolli et al., 2011;
31 Papa et al., 2013; Peres and Cancelliere, 2014; Posner and Georgakakos, 2015; Greco
32 and Bogaard; 2016), which can be useful for carrying out stochastic predictions.
33 However, the application of such physically based approaches in operational early
34 warning systems still suffers the involved computational burden, which makes
35 difficult carrying out in real time the calculations required for landslide probability
36 assessment. Consequently, empirical models of the relationship between rainfall and

slope stability are still preferred for early warning purposes (Sirangelo and Braca, 2004; Greco et al., 2013; Manconi and Giordan, 2016; Ozturk et al., 2016).

An example of setting up an early warning predictive tool taking into account the uncertainty of the prediction has been developed by coupling a stochastic predictive model of precipitations (Giorgio and Greco, 2009) with the empirical model FLaiR (Sirangelo and Versace, 1996), which yields predictions of the triggering time for rainfall-induced landslides.

The FLaiR model associates landslide triggering conditions with values of a mobility function $Y(t)$, obtained by a convolution integral of the rainfall history $R(t)$ with a suitable transfer function $\psi(t)$, which allows to model a wide variety of geomorphological contexts, taking into account predisposing conditions generated by antecedent rainfalls (Iiritano et al., 1998; Sirangelo et al., 2003).

The choice of the transfer function and calibration of its parameters are carried out based on the historical rainfalls data records in a way that the $Y(t)$ function may result as a suitable indicator of slope stability conditions. In particular, parameters are calibrated so that peaks of $Y(t)$ correspond to historical landslides, so to identify a threshold Y_{cr} that, if exceeded, indicates landslide occurrence.

The FLaiR model is currently implemented as predictive model in early warning systems provided for different thresholds of attention, alert and alarm, corresponding to a progressive approach of $Y(t)$ to the Y_{cr} threshold. As an example, for the case of Sarno (pyroclastic slopes in southern Italy) the three mentioned thresholds were suggested at values of $0.4Y_{cr}$, $0.6Y_{cr}$ and $0.8Y_{cr}$, respectively.

The coupling with a stochastic predictive model of rainfall allows adopting the FLaiR model as a predictor of the probability of occurrence of future landslides (Capparelli et al., 2013). In fact, the convolution integral may be separated into two parts, one deterministic, the other random. The first integral computes the convolution of the rainfall history $R_{obs}(t)$ until the time at which the prediction is carried out. The second integral computes the convolution of the rainfall history $R_{pre}(t)$ predicted for the future time interval t_{pre} , the upper bound of which represents the lead time of the prediction:

$$Y(t) = Y_{det} + Y_{pre} = \int_{-\infty}^{t-t_{pre}} \Psi(t-\tau) R_{obs}(\tau) d\tau + \int_{t-t_{pre}}^t \Psi(t-\tau) R_{pre}(\tau) d\tau \quad (1)$$

The prediction of Y_{pre} is carried out by evaluating the probability conditioned to the trend of the rainfall observed before prediction. To this aim, the model DRIP (Disaggregated Rectangular Intensity Pulse) is adopted (Heneker et al., 2001). It

1 defines, through an alternating renewal process, the observed alternation of rainfall
2 and dry periods. This process guarantees, in fact, the stochastic independence of a
3 rainfall event from the duration of the immediately preceding dry period as well as
4 from the duration and the total rainfall height of the previous rainstorm. This allows
5 carrying out the conditioned prediction Y_{pre} by only taking into account the rainfall
6 history observed during the current event, when the prediction is being carried out.

7 The prediction Y_{pre} is carried out by a non-parametric approach, by selecting within
8 the historical data set only the N_i rainfall events meeting the following conditions:
9 their duration was equal or longer than the observed part of the current rainstorm;
10 along a time interval as long as the lead time, t_{pre} , before the prediction, the mobility
11 function increased in the same proportion as it occurred during the last observed t_{pre}
12 interval of the current rainfall event.

13 The rainfall events selected by following this procedure allow computing the expected
14 value of Y_{pre} and the probability that, at the end of the interval t_{pre} , the condition $Y > Y^*$
15 occurs, whatever Y^* . Hence, once alert and alarm thresholds of the mobility function
16 are defined, the sensitivity of the early warning system can be adjusted by setting up
17 the probability of threshold exceedance at which the relevant messages are launched
18 (activation probability), so to obtain the best trade-off between false and missing
19 alarms (Greco et al., 2013). Low values of the activation probabilities result in high
20 number of alerts and alarms, and may lead to wrong activations of the system (false
21 alert/alarms). Conversely, a less sensitive system unavoidably increases the number
22 of erroneous non-activations of the system (missing alerts-alarms).

23 The choice of the more suitable values at which setting the activation probabilities
24 represents an important and crucial feature in the setting of an effective early
25 warning system. As already specified previously, the system sensitivity has to take
26 into account all consequences relating with false and missing alarms. For the alert
27 level, it is usually better to set a high sensitivity, since actions determined by alert
28 activations usually do not imply high costs, nor a significant involvement of the served
29 community. The same, however, cannot be stated for the alarm level, as the
30 procedures resulting from alarm spread usually imply high costs and discomfort for
31 the community. As an example, evacuation of people involve stopping all activities
32 and interruption of all infrastructures and services of public utility.

33 The described approach has been applied to the slope of Pessinetto, 40 km North-
34 East of Turin. The slope, oriented towards South-West, with inclination angle between
35 30° and 35°, is part of the watershed of the river Stura di Lanzo. It is constituted by a
36 metamorphic bed-rock intensively fractured, covered by a clayey-silt. Six debris flows



1 of different volumes occurred there, within an area of about 1 km², from November
2 1962 to October 2000. The thickness of mobilized soils ranged between 1.5 and 2.0
3 m, with soil volumes ranging between few hundreds to 10000 m³.

4 For the calibration of the stochastic model and of the alert system, the pluviometer
5 data recorded in Lanzo, located 6.5 km east of the slope, were available. Particular,
6 the calibration has been carried out by interpreting the hourly precipitations recorded
7 between 1 January 1956 and 10 September 1991. Subsequent data, from 11
8 September 1991 to 15 June 2004, have been adopted to validate the predictions.

9 The critical value for the mobility function, estimated over the calibration period, was
10 $Y_{cr}=168.4$ mm/days.

11 The minimum duration of a dry period in-between two rainfall events has been set
12 equal to 10 hours. By assuming only rainfall events exceeding 5 mm to be significant
13 for early warning purposes, a series of 1102 rainfall events meeting the requirements
14 in terms of stochastic independency was selected within the calibration period. These
15 selected events were characterized by durations between 1 hour and 182 hours and
16 rainfall heights between 5 mm and 615 mm (Greco et al., 2013).

17 The validation period of the early warning system included 456 rainstorms with
18 rainfall heights exceeding 5 mm.

19 The EWS has been implemented through the definition of two different operational
20 levels: an alert level and an alarm level. The alert triggers as soon as the mobility
21 function is predicted to approach the value of $Y_a=0.75Y_{cr}$ with a probability higher than
22 a predefined threshold P_1 . The alarm is spread when the probability that Y exceeds
23 the critical value Y_{cr} is higher than a second threshold P_2 . Predictions are updated with
24 a hourly frequency and refer to a time interval from 1 to 6 hours later than the
25 prediction time.

26 Two examples of the potentiality of the predictions of the probability of exceeding
27 the two defined thresholds are given for two rainfall events occurred during the
28 validation period, both followed by landslides. In particular, the reported predictions
29 were carried out with lead times of up to 5 hours.

30 The first event occurred between 22 and 25 September 1993, and Y_a and Y_{cr} were
31 overtaken 54 and 58 hours after the beginning of the rain, respectively. A landslide
32 was triggered after 60 hours. In the second example, a rainfall event occurred
33 between the 12 and 15 October 2000, Y_a was passed 39 hours after the beginning of
34 the rain storm, Y_{cr} after 45 hours, and the landslide occurred after 46 hours.

1 The effectiveness of the stochastic approach for early warning is shown in figures 4
2 and 5. The graphs give the probability of exceeding the alert and alarm thresholds in
3 the following five hours, predicted in real time. During the two considered rainfall
4 events, the system predicted high values of the probability of exceeding both
5 thresholds several hours in advance. In particular, assuming the activation
6 probabilities $P_1=P_2=0.3$, in both cases (25 September 1993, figure 4; 14 October 2000,
7 figure 5) the alert would have been issued about 9 hours before the landslide, while
8 the alarm would have been launched already 6 hours earlier than the triggering time.


9 Hence, by properly setting P_1 and P_2 , the EWS would have been capable to launch, in
10 both cases, the alert and alarm messages several hours before the actual landslide
11 triggering. Tables 1 and 2 show the influence of different choices for P_1 and P_2 on the
12 performance of the EWS, evaluated in terms of total numbers of missing and false
13 alerts and alarms during the entire validation period. It looks clear how the sensitivity
14 of the early warning system depends on the chosen activation probability: higher
15 probabilities correspond to larger numbers of missing alarms, and smaller numbers
16 of false alarms.

17 The optimal choice of P_1 and P_2 should be identified by comparing the costs deriving
18 from false and missing alerts and alarms, with the benefits of the true alarms. As
19 already pointed out in the previous sections, such a cost-benefit analysis is of course
20 peculiar of the particular considered case.

21 The capability of spreading the alert some hours earlier than the triggering time is a
22 non-trivial feature of the system, when it is implemented to mitigate risks from
23 phenomena characterized by a very rapid evolution, such as debris flows and other
24 types of fast landslides, as well as flash floods. In these cases, effective measures to
25 prevent damages and victims may be successfully implemented only if the alarm is
26 spread sufficiently earlier than the triggering time of the phenomenon.

27

28 **Physically based approach**

29 In the town of Nocera Inferiore a  **second** pluviometer, installed in 1997, recorded
30 hourly rainfalls near the slope where on 4 March 2005 the sadly famous landslide of
31 Nocera Inferiore was triggered (Figure 6). The slope was tilted at 40° and covered with
32 a 2 meters thick layer of silty volcanic soils. Rainfall records are adopted in this
33 example to validate a physically based approach (Pagano et al., 2010), suitable to take
34 into account a number of known influencing factors (triggering event, antecedent

precipitation, instantaneous rainfall intensity, evolution of potential infiltration)(Pagano et al., 2008; Rianna et al., 2014a).

~~The modelling of the boundary value problem~~ has been simplified as much as possible, but without determining excessive loss in prediction reliability. Only some factors, considered of minor importance ~~for the problem in hand~~, were disregarded, according to Pagano et al. (2010). In particular, a one-dimensional infiltration ~~problem~~ through an unsaturated rigid medium was set through Richards equations, solved by the FEM code SEEP/W (GEOSLOPE 2004).

Hourly rainfall records were adopted to quantify boundary fluxes at the uppermost boundary, while at the lowermost boundary two different limit boundary conditions were assumed (Reder et al., 2017) to account for the possible effects exerted by the fractured bedrock on the silty volcanic cover: a seepage surface condition, which simulates the capillary barrier effect in the hypothesis that fractures are empty; a flux regulated by the unit gradient, which instead approaches the case of fractures filled with the same material as that constituting the cover. The hydraulic properties of the soil, i.e. water retention curve and hydraulic conductivity function, were obtained by means of laboratory tests (Nicotera& Papa, 2007) as well as by coupled measurements of soil matric suction (Jetfill tensiometers) and volumetric water content (TDR) carried out in a lysimeter (Rianna et al., 2014b).

Results yielded by the analyses (Reder et al., 2017) in terms of suction evolution refer to the hydrological year 2004-2005 (Figure 7), which includes the landslide event. They clearly show how the predictions indicates a singularity at the triggering time, consisting in a drop of suction throughout the cover below 3kPa for both boundary condition-types assumed at the bottom. Analyses conducted for the whole historical series of recorded rainfalls, covering a time interval of 10 years including the landslide (Pagano et al., 2010), indicate that the same singularity is yielded by the prediction only once more. Hence, if this singularity (suction below 3 kPa throughout the cover) had been adopted as an alarm criterion, the number of false alarms would have resulted significantly low. Furthermore, the short time required to update the prediction (few minutes) is consistent with the requirement of promptness of an early warning system and allows carrying out “in line” predictions.

6. CONCLUSIONS

The paper summarizes the essential elements of early warning systems, implemented for a real time and continuous check of safety conditions with regard to catastrophic

natural phenomena, in order to accomplish a mitigation of the associated risk. In case of prediction of a paroxysmal phenomenon, the system should start a procedure leading to the prompt activation of measures for the protection of exposed goods and people. In particular, the paper highlights the need for detailed knowledge of how the different stages of the phenomenon develop over time and, in general, of the factors affecting each stage. Both these requirements are crucial, in order to establish at which stage the early warning prediction should be implemented to maximize its effectiveness.

With reference to two different phenomena, namely flow-like landslide and earth flows, both characterized by rapid evolution, the paper describes, by means of three examples, some alternative approaches to the development of the predictive tool and to its implementation in an EWS.

References

Alfieri L., Salamon P., Pappenberger F., Wetterhall F., Thielen J.: Operational early warning systems for water-related hazards in Europe. *Environmental Science & Policy*, 21, 35–49, <http://dx.doi.org/10.1016/j.envsci.2012.01.008>, 2012

Alfieri L., Thielen J.: A European precipitation index for extreme rain-storm and flash **flood early** warning. *Meteorological Applications*, 22: 3–13, <http://dx.doi.org/10.1002/met.1328>, 2015

Arnone E., Noto L.V., Lepore C., Bras R.L.: Physically-based and distributed approach to analyze rainfall-triggered landslides **at watershed** scale, *Geomorphology*, 133, 121–131, <http://dx.doi.org/10.1016/j.geomorph.2011.03.019>, 2011

BAKKEHOI S.: Snow avalanche prediction using a probabilistic method. *Avalanche Formation, Movement and Effects*, Proceedings of the Davos Symposium, September 1986, IAHS Publ. 162, 1986

Baum R.L., Godt J.W.: Early warning of rainfall-induced shallow landslides **and debris** flows in the USA, *Landslides*, 7(3), 259–272, <http://dx.doi.org/10.1007/s10346-009-0177-0>, 2010

Calcaterra D., de Riso R., Evangelista A., et al.: Slope instabilities in the pyroclastic deposits of the Phlegraean district and the carbonate Apennine (Campania, Italy), *Proceedings of an International Workshop on Occurrence and Mechanisms of Flows in Natural Slopes and Earthfills held in Sorrento, Italy, 14-16 May 2003*, 61–75, 2004

1 Capparelli G., Giorgio M., Greco R.: Shallow Landslides Risk Mitigation by Early
2 Warning: The Sarno Case, Margottini et al (eds), Landslide Science and Practice,
3 Springer-Verlag, Berlin, 6, 767-772, <http://dx.doi.org/10.1007/978-3-642-31319-698>,
4 2013

5 Capparelli G., Versace P.: FLAIR and SUSHI: two mathematical models for early
6 warning of landslides induced by rainfall, Landslides, 8(1), 67-79,
7 <http://dx.doi.org/10.1007/s10346-010-0228-6>, 2011

8 Cascini L., Ferlisi S.: Occurrence and consequences of flowslides: a case study,
9 Proceedings of an International Conference on Fast Slope Movements – Prediction
10 and Prevention for Risk Mitigation held in Napoli, 11-13 May 2003, 1, 85-92, 2003

11 Chleborad A.F., Baum R.L., Godt J.W.: A prototype system for forecasting **landslides** in
12 the Seattle, Washington, area, Baum R.L., Godt J.W., Highland L.M. (Eds.), Engineering
13 geology and landslides of the Seattle, Washington, area, Geological Society of
14 America Reviews in Engineering Geology, Geological Society of America, Boulder, XX,
15 103–120, [http://dx.doi.org/10.1130/2008.4020\(06\)](http://dx.doi.org/10.1130/2008.4020(06)), 2008

16 Cranston M.D., Tavendale A.C.W.: Advances in operational flood forecasting in
17 Scotland, Proceedings of the Institution of Civil Engineers - Water Management,
18 165(2), 69-87, <http://doi.org/10.1680/wama.2012.165.2.79>, 2012

19 de Saint-Aubin C., Garandeau L., Janet B., Javelle P.: A new French flash flood
20 warning service, Samuels P, Klijn F, Lang M (Eds.), E3S Web of Conferences, 3rd
21 European Conference on Flood Risk Management, FLOODrisk 2016, Lyon, France, 17-
22 21 October 2016, EDP Sciences, Les Ulis, 7, 18-24,
23 <http://doi.org/10.1051/e3sconf/20160718024>, 2016

24 Eichenberger J., Ferrari A., Laloui L.: Early warning thresholds for partially saturated
25 slopes in volcanic ashes, Computers and Geotechnics, 49, 79–89,
26 <http://dx.doi.org/10.1016/j.compgeo.2012.11.002>, 2013

27 GEO-SLOPE: SEEP/W for finite element seepage analysis, GEO-SLOPE International,
28 Calgary, 2004

29 Giorgio M., Greco R.: Rainfall height stochastic modelling as a support tool for floods
30 and **flowslides** **earlywarning**, Water Engineering for a Sustainable Environment,
31 Proceedings of XXXIII IAHR Congress. Vancouver, International Association of
32 Hydraulic Engineering & Research, August 2009, 6812-6819, 2009

33 Greco R., Bogaard T.A.: The influence of non-linear hydraulic behavior of slope soil
34 covers on rainfall intensity-duration thresholds, S. Aversa et al (eds), Landslides and

1 Engineered Slopes. Experience, Theory and Practice, 2, 1021-1025, Taylor and Francis,
2 2016

3 Greco R., Giorgio M., Capparelli G., Versace P.: Early warning of rainfall-induced
4 landslides based on empirical mobilityfunction predictor, Engineering Geology, 153,
5 68-79.[http, //dx.doi.org/10.1016/j.enggeo.2012.11.009](http://dx.doi.org/10.1016/j.enggeo.2012.11.009), 2013

6 Guzzetti F., Peruccacci S., Rossi M., Stark C.P.: Rainfall thresholds for the **initiationof**
7 landslides in central and southern Europe. Meteorology and **AtmosphericPhysics**, 98,
8 239–267, <http://dx.doi.org/10.1007/s00703-007-0262-7>, 2007

9 Guzzetti F., Peruccacci S., Rossi M., Stark C.P.: The rainfall intensity-**durationcontrol** of
10 shallow landslides and debris flows: an update, Landslides, 5, 3–17,
11 <http://dx.doi.org/10.1007/s10346-007-0112-1>, 2008

12 Heneker T.M., Lambert M.F., Kuczera G.: A point rainfall model for risk-**baseddesign**.
13 Journal of Hydrology, 247 (1–2), 54–71, [http://dx.doi.org/10.1016/S0022-](http://dx.doi.org/10.1016/S0022-1694(01)00361-4)
14 [1694\(01\)00361-4](http://dx.doi.org/10.1016/S0022-1694(01)00361-4), 2001

15 Iadanza C., Trigila A., Napolitano F.: Identification and characterization of rainfall
16 events responsible for triggering of debris flows and shallow landslides, Journal of
17 Hydrology, 541, 230-245, <http://dx.doi.org/10.1016/j.jhydrol.2016.01.018>, 2016

18 Iiritano G., Versace P., Sirangelo B.: Real-time estimation of hazard for landslides
19 triggered byrainfall, Environmental Geology, 35(2-3), 175-183,
20 <http://dx.doi.org/10.1007/s002540050303>, 1998

21 Jakob M., Owen T., Simpson T.: A regional real-time debris-flow warning **systemfor**
22 the District of North Vancouver, Canada, Landslides, 9, 165–178,
23 <http://dx.doi.org/10.1007/s10346-011-0282-8>, 2012

24 Keefer D.K., Wilson R.C., Mark R.K., Brabb E.E., Brown W.M., Ellen S.D., Harp E.L.,
25 Wieczorek G.F., Alger C.S., Zatzkin R.S.: Real-time landslide warning **duringheavy**
26 rainfall, Science, 238, 921–925, <http://dx.doi.org/10.1126/science.238.4829.921>,
27 1987

28 Liu X., Liu Y., Li L., Ren Y.: Disaster monitoring and early-warning system for snow
29 avalanche along Tianshan highway, IEEE International Geoscience and
30 **RemoteSensing** Symposium, IGARSS 2009, Cape Town. South Africa; 12-17 July 2009,
31 IEEEGeoscience and Remote Sensing Society, 2, 11634-11637,
32 <http://dx.doi.org/10.1109/IGARSS.2009.5418166>, 2009

33 Ma H., Chi F.: Major Technologies for Safe Construction of High Earth-Rockfill Dams,
34 Engineering 2, 498–509, <http://dx.doi.org/10.1016/J.ENG.2016.04.001>, 2016

- 1 Manconi A., Giordan D.: Landslide failure forecast in near-real-time. *Geomatics,*
2 *Natural Hazards and Risk,* 7(2), 639-648,
3 <http://dx.doi.org/10.1080/19475705.2014.942388>, 2016
- 4 Mannara G., Sarnataro A., Sposito P., Piccolo G., Ciancia N., Infante S.: Rete di sensori
5 accelerometrici MEMS per il monitoraggio in continuo di rilievi franosi in ambito
6 ferroviario, SEF09 Sicurezza ed Esercizio Ferroviario I Convegno Nazionale, Roma 20
7 marzo 2009, 2009 (in Italian)
- 8 Maugeri M., Motta E.: Slope Failure. Effects of Heavy Rainfalls on Slope Behavior: The
9 October 1, 2009 Disaster of Messina (Italy), Iai S. (eds) *Geotechnics and Earthquake*
10 *Geotechnics Towards Global Sustainability*, Geotechnical, Geological, and Earthquake
11 Engineering, Springer, Dordrecht, 15, 2011
- 12 Michoud C., Bazin S., Blikra L.H., Derron M.H., Jaboyedoff M.: Experiences from site-
13 specific landslide early warning systems, *Natural Hazards and Earth System Sciences,*
14 13, 2659-2673, <http://dx.doi.org/10.5194/nhess-13-2659-2013>, 2013
- 15 Ortigao B., Justi M.G. 2004: Rio-Watch: the Rio de Janeiro landslide alarm
16 system. *Geotechnical News*, 22(3), 28–31, 2013
- 17 Nicotera M., Papa R.: Comportamento idraulico e meccanico della serie piroclastica
18 di Monteforte Irpino, Progetto PETIT-OSA Monitoraggio Frane: Contributo alle
19 Conoscenze sulla Franosità in Campania, 272-280. ARACNE, 2007
- 20 Ozturk U., Tarakegn Y.A., Longoni L., Brambilla D., Papini M., Jensen J.: A simplified
21 early-warning system for imminent landslide prediction based on failure index
22 fragility curves developed through numerical analysis, *Geomatics, Natural Hazards*
23 *and Risk*, 7(4), 1406-1425, <http://dx.doi.org/10.1080/19475705.2015.1058863>, 2016
- 24 Pagano L.; Picarelli L.; Rianna G.; Urciuoli G.: A simple numerical procedure for
25 timely prediction of precipitation-induced landslides in unsaturated pyroclastic soils,
26 *Landslides*, 7, 273 - 289, 2010
- 27 Pagano L., Zingariello M.C., Vinale F.: A large physical model to simulate flowslides in
28 pyroclastic soils, *Proc First European Conf on Unsaturated Soils: Advances in Geo-*
29 *Engineering*, Durham, 205-213, 2008
- 30 Pagano L., Sica S.: Earthquake Early Warning for Earth Dams: Concepts and
31 Objectives. *Natural Hazards*, 66, 303 – 318, [http://dx.doi.org/10.1007/s11069-012-](http://dx.doi.org/10.1007/s11069-012-0486-9)
32 [0486-9](http://dx.doi.org/10.1007/s11069-012-0486-9), 2013
- 33 Papa M.N., Medina V., Ciervo F., Bateman A.: Derivation of critical rainfall thresholds
34 for shallow landslides as a tool for debris flow early warning systems, *Hydrology and*

1 Earth System Sciences, 17, 4095–4107, [http://dx.doi.org/10.5194/hess-17-4095-](http://dx.doi.org/10.5194/hess-17-4095-2013)
2 2013, 2013

3 Peres D.J., Cancelliere A.: Derivation and evaluation of landslide-triggering thresholds
4 bya Monte Carlo approach, Hydrology and Earth System Sciences, 18, 4913–4931,
5 <http://dx.doi.org/10.5194/hess-18-4913-2014>, 2014

6 Ponziani F., Pandolfo C., Stelluti M., Berni N., Brocca L., Moramarco T.: Assessment of
7 rainfall thresholds and soil moisture modeling for operational hydrogeological
8 riskprevention in the Umbria region (central Italy), Landslides, 9, 229–237,
9 <http://dx.doi.org/10.1007/s10346-011-0287-3>, 2012

10 Posner A.J., Georgakakos K.P.: Soil moisture and precipitation thresholds for real-
11 **timelandslide** prediction in El Salvador, Landslides, 12, 1179–1196,
12 <http://dx.doi.org/10.1007/s10346-015-0618-x>, 2015

13 Pumo D., Francipane A., Lo Conti F., Arnone E., Bitonto P., Viola F., La Loggia G., Noto
14 L.V.: The SESAMO early warning system for rainfall-triggered landslides, Journal of
15 Hydroinformatics, 18(2), 256-276, <http://dx.doi.org/10.2166/hydro.2015.060>, 2016

16 Rabuffetti D., Barbero S.: Operational hydro-meteorological warning and real-time
17 flood forecasting: the Piemonte Region case study, Hydrology and Earth System
18 Sciences, 9, 457-466. <https://doi.org/10.5194/hess-9-457-2005>, 2005

19 Reder A., Pagano, L., Picarelli, L., Rianna G.: The role of the lowermost boundary
20 conditions in the hydrological response of shallow sloping covers, Landslides 14, 3,
21 861-873; <https://doi.org/10.1007/s10346-016-0753-z>, 2017

22 Rianna G., Pagano L., Urciuoli G.: Rainfall patterns triggering shallow flowslides in
23 pyroclastic soils, Engineering Geology 174, 22- 35, 2014a

24 Rianna G., Pagano L., Urciuoli G.: Investigation of soil-atmosphere interaction in
25 pyroclastic soils, Journal of Hydrology 510, 480-492, 2014b

26 Ruiz-Villanueva V., Bodoque J.M., Díez-Herrero A., Calvo C.: Triggering threshold
27 precipitation and soil hydrological characteristics of shallowlandslides in granitic
28 landscapes, Geomorphology, 133, 178-189,
29 <http://dx.doi.org/10.1016/j.geomorph.2011.05.018>, 2011

30 Santo A., Di Crescenzo G., Del Prete S., Di Iorio L.: The Ischia island flash flood of
31 November 2009 (Italy): Phenomenon analysis and flood hazard. Physics and
32 Chemistry of the Earth, Parts A/B/C, 3-17, [49](https://doi.org/10.1016/j.pce.2011.12.004),
33 <https://doi.org/10.1016/j.pce.2011.12.004>, 2012

1 Schmidt J., Turek G., Clark M.P., Uddstrom M., Dymond J.R.: Probabilistic forecasting
2 of shallow, rainfall-triggered landslides using real-time numerical weather predictions,
3 Natural Hazards and Earth System Sciences, 8: 349–357,
4 <http://dx.doi.org/10.5194/nhess-8-349-2008>, 2008

5 Segoni S., Battistini A., Rossi G., Rosi A., Lagomarsino D., Catani F., Moretti S., Casagli
6 N.: Technical Note: An operational landslide early warning system at regional scale
7 based on space–time-variable rainfall thresholds, Natural Hazards and Earth System
8 Sciences, 15, 853–861, <http://dx.doi.org/10.5194/nhess-15-853-2015>, 2015

9 Sirangelo B., Braca G.: Identification of hazard conditions for mudflow occurrence by
10 hydrological model. Application of FLAIR model to Sarno warning system, Engineering
11 Geology, 73, 267–276, <http://dx.doi.org/10.1016/j.enggeo.2004.01.008>, 2004

12 Sirangelo B., Versace P.: A real time forecasting model for landslides triggered by
13 rainfall, Meccanica, 31(1), 73–85, <http://dx.doi.org/10.1007/BF00444156>, 1996

14 Sirangelo B., Versace P., Capparelli G.: Forwarning model for landslides triggered by
15 rainfall based on the analysis of historical data file, Servat E., Najem W., Leduc C.,
16 Shakeel A. (eds.), Hydrology of the Mediterranean and Semiarid Regions, IAHS Publ.,
17 278, 298–304, 2003

18 Tarolli P., Borga M., Chang K.T., Chiang S.H.: Modeling shallow landsliding
19 susceptibility by incorporating heavy rainfall statistical properties. Geomorphology,
20 133, 199–211, <http://dx.doi.org/10.1016/j.geomorph.2011.02.033>, 2011

21 Terlien M.T.J.: The determination of statistical and deterministic hydrological
22 landslide-triggering thresholds, Environmental Geology, 35(2–3), 124–130,
23 <http://dx.doi.org/10.1007/s002540050299>, 1998

24 Tiranti D., Rabuffetti D. Estimation of rainfall thresholds triggering shallow landslides
25 for an operational warning system implementation, Landslides, 7, 471–481,
26 <http://dx.doi.org/10.1007/s10346-010-0198-8>, 2010

27 UN-ISDR (United Nations International Strategy for Disaster Reduction): Hyogo
28 framework for action 2005–2015: building the resilience of nations and communities
29 to disasters, World Conference on Disaster Reduction, Kobe, Japan, January 2005
30 (<http://www.unisdr.org/eng/hfa/docs/Hyogo-framework-foraction-english.pdf>),
31 2005

d_{pre} [h]	$P_1=0.2$			$P_1=0.25$			$P_1=0.3$		
	N_{1L}	N_{1F}	N_{1M}	N_{1L}	N_{1F}	N_{1M}	N_{1L}	N_{1F}	N_{1M}
2	23	7	2	19	3	2	18	2	2
4	27	11	3	22	7	4	21	6	4
6	31	12	3	25	7	4	22	5	5

Table 1

d_{pre} [h]	$P_2=0.2$			$P_2=0.25$			$P_2=0.3$		
	N_{2L}	N_{2F}	N_{2M}	N_{2L}	N_{2F}	N_{2M}	N_{2L}	N_{2F}	N_{2M}
2	16	4	0	14	2	0	11	1	2
4	22	10	0	17	5	0	15	4	1
6	29	16	1	20	7	1	13	4	5

Table 2

1 CAPTIONS

2 Figure 1. Evolution stages of a collapse mechanism

3 Figure 2. Evolution stages of collapse mechanism in rainfall-induced landslides
4 featured by rapid kinematic

5 Figure 3 - Daily and antecedent-bi-monthly rainfalls recorded at the Nocera Inferiore
6 site and corresponding to significant events (red circles are associated with landslide
7 triggering, green circle with rainfall histories similar to those resulting in landslides)

8
9 Figure 4. Stochastic approach to early warning: probability of exceeding alert and
10 alarm thresholds of the mobility function at the slope of Pessinetto, predicted in real
11 time (the upper panel reports the observed hyetograph) during the storm of
12 22.09.1993, when an earth flow occurred 60 hours after the beginning of the rain.

13
14 Figure 5. Stochastic approach to early warning: probability of exceeding alert and
15 alarm thresholds of the mobility function at the slope of Pessinetto, predicted in real
16 time (the upper panel reports the observed hyetograph) during the storm of
17 12.10.2000, when an earth flow occurred 46 hours after the beginning of the rain.

18
19 Figure 6. The Nocera Inferiore 2005 landslide area (Pagano et al., 2010, modified)

1 Figure 7. Prediction of suction evolution over the hydrological year of the Nocera
2 Inferiore 2005 landslide at four different depths and for two different hydraulic
3 conditions at the lowermost boundary (Reder et al., 2017, modified)

4

5 Table 1. Stochastic approach to early warning: numbers of launched (N_{1L}), false (N_{1F})
6 and missing (N_{1M}) alerts at the slope of Pessinetto for three different lead times t_{pre}
7 and three different choices of the probability of alert activation P_1 . For each lead time,
8 the system carried out 964 predictions between 11 September 1991 and 15 June 2004
9 (validation period).

10

11 Table 2. Stochastic approach to early warning: numbers of launched (N_{2L}), false (N_{2F})
12 and missing (N_{2M}) alarms at the slope of Pessinetto for three different lead times t_{pre}
13 and three different choices of the probability of alarm activation P_2 . For each lead
14 time, the system carried out 964 predictions between 11 September 1991 and 15 June
15 2004 (validation period).

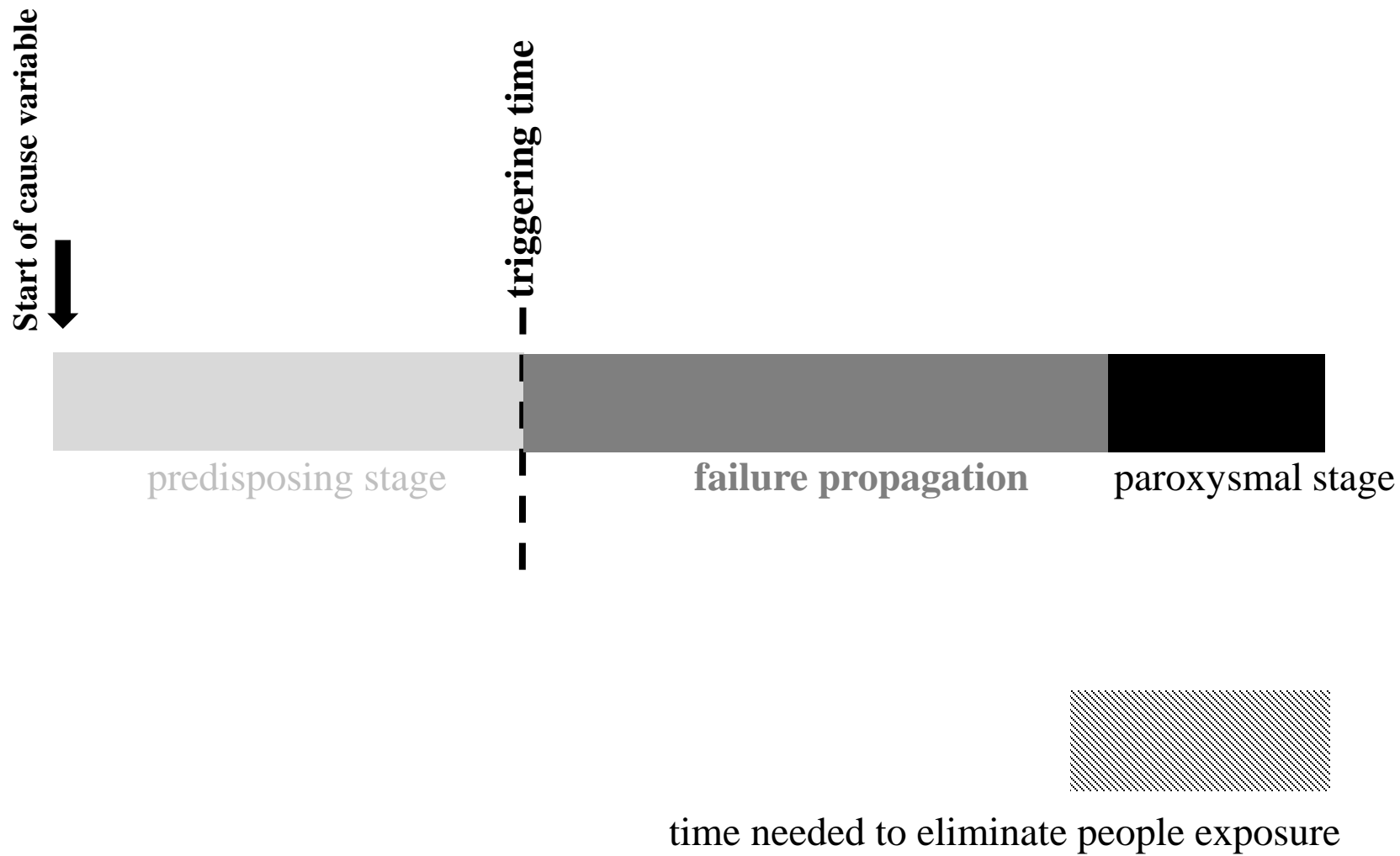


Figure 1

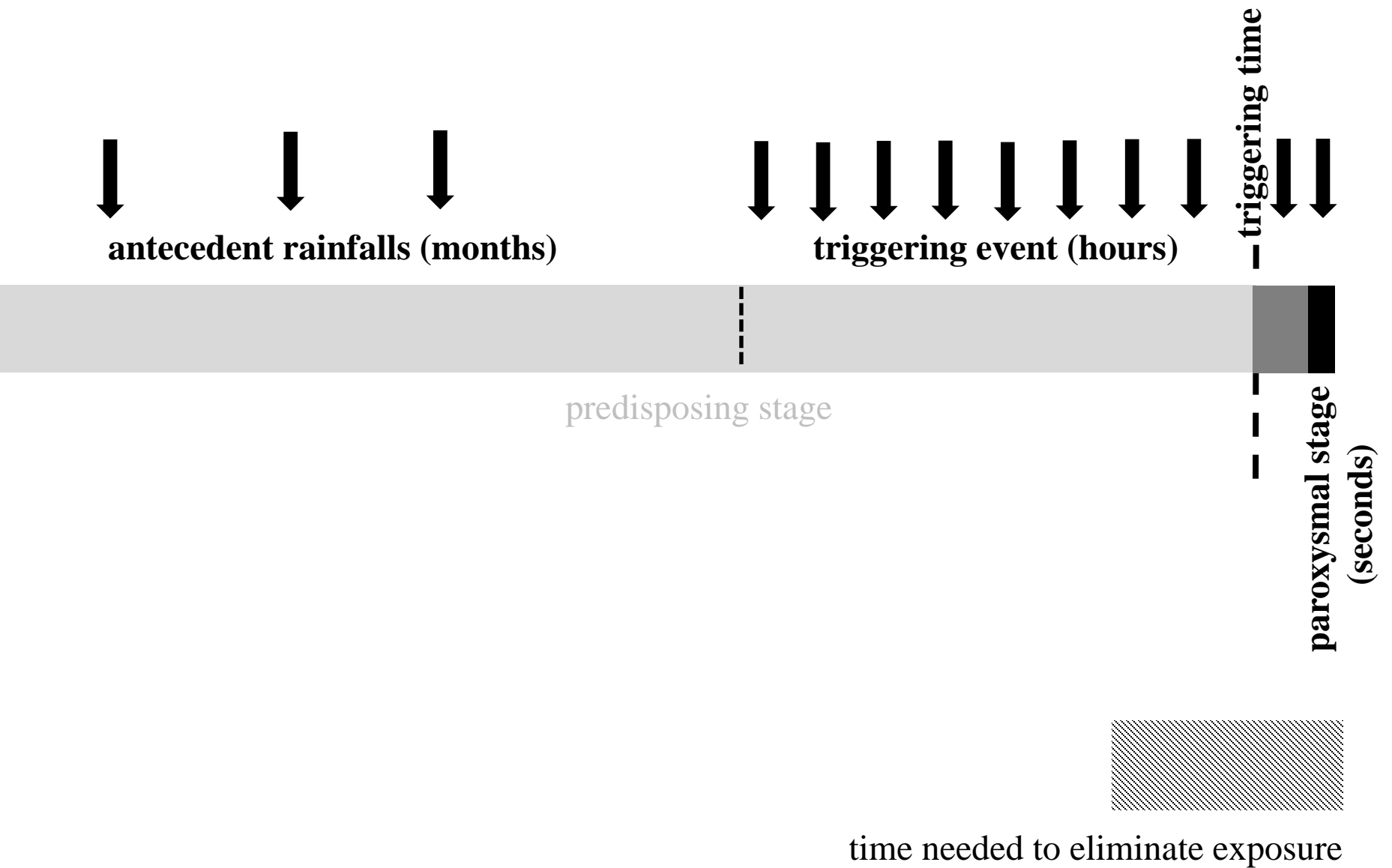


Figure 2

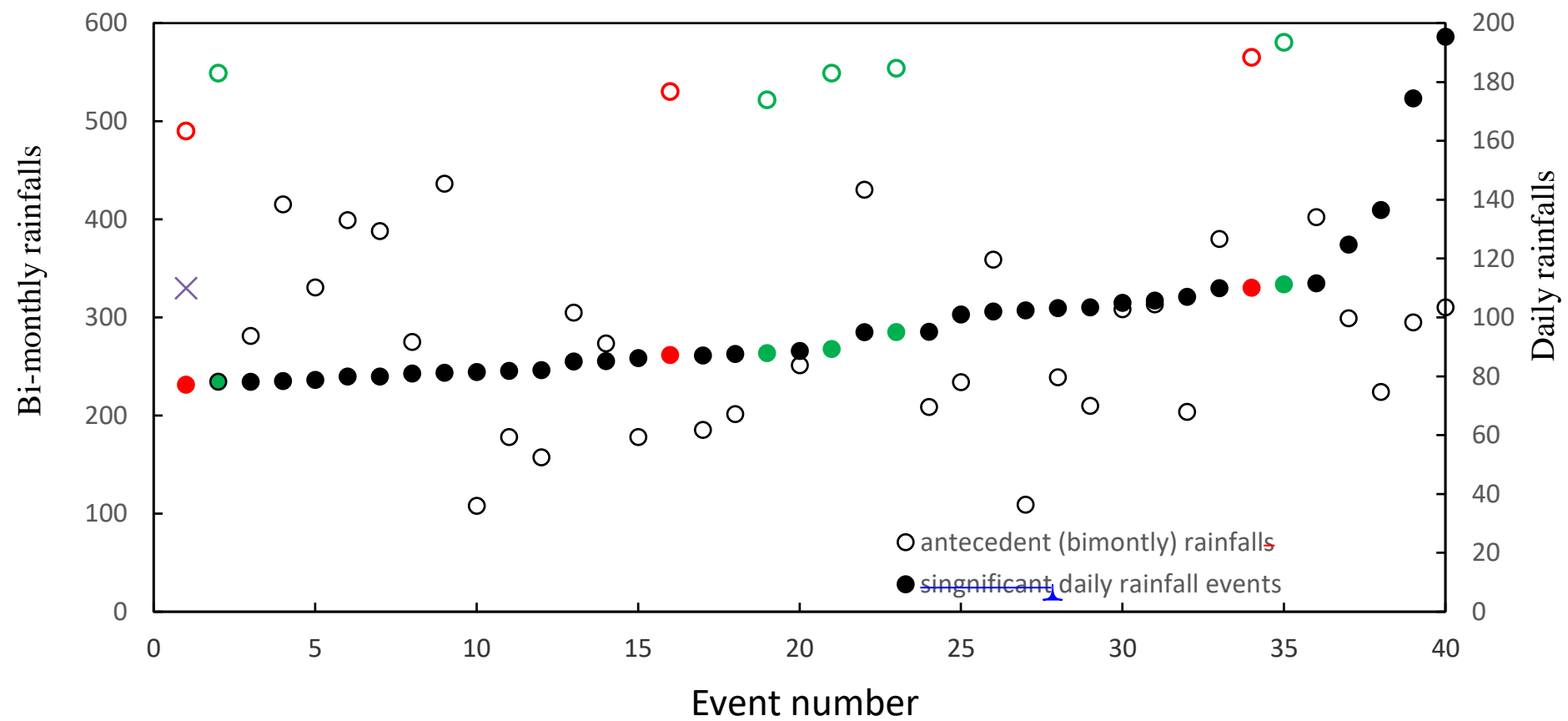


Figure 3

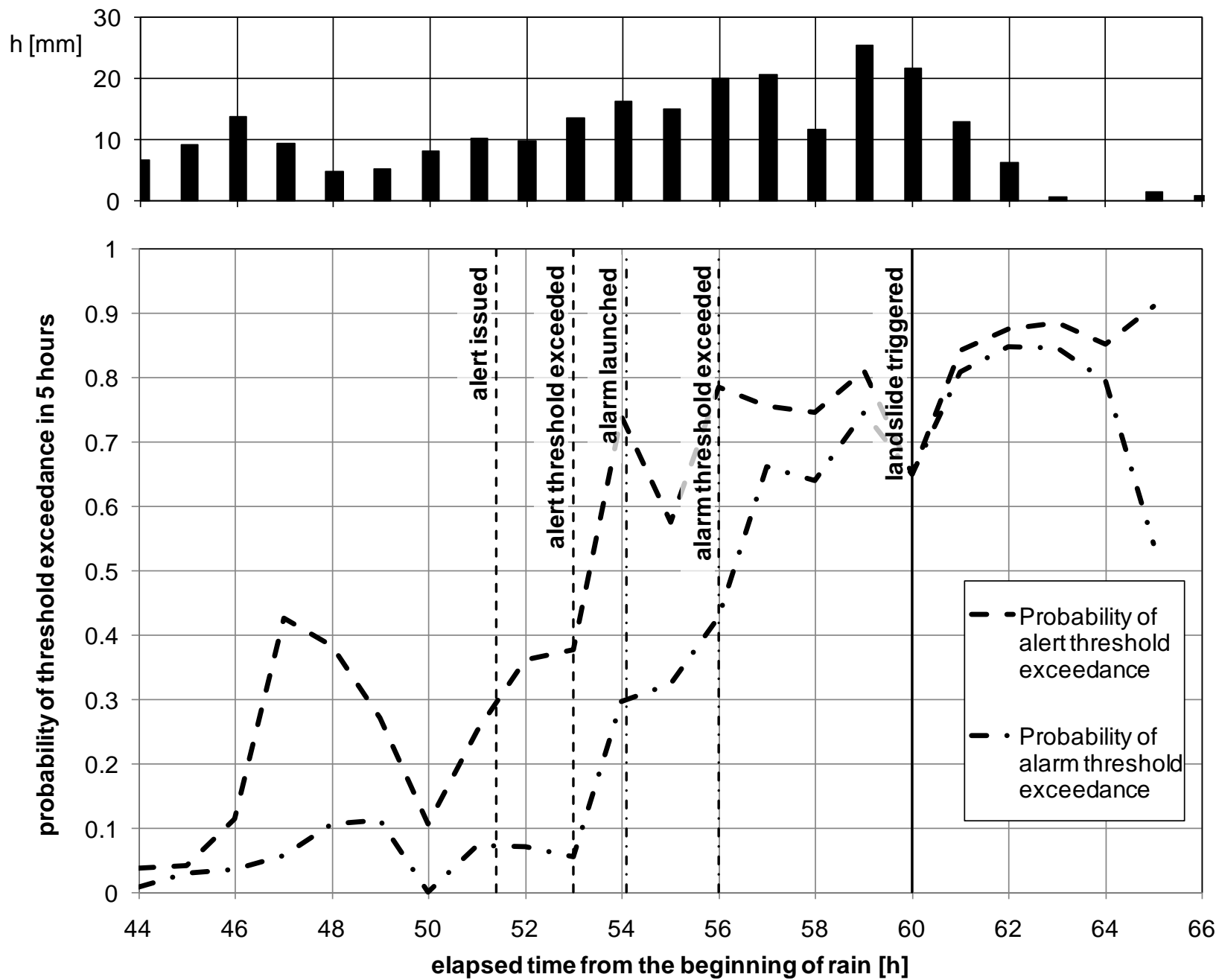


Figure 4

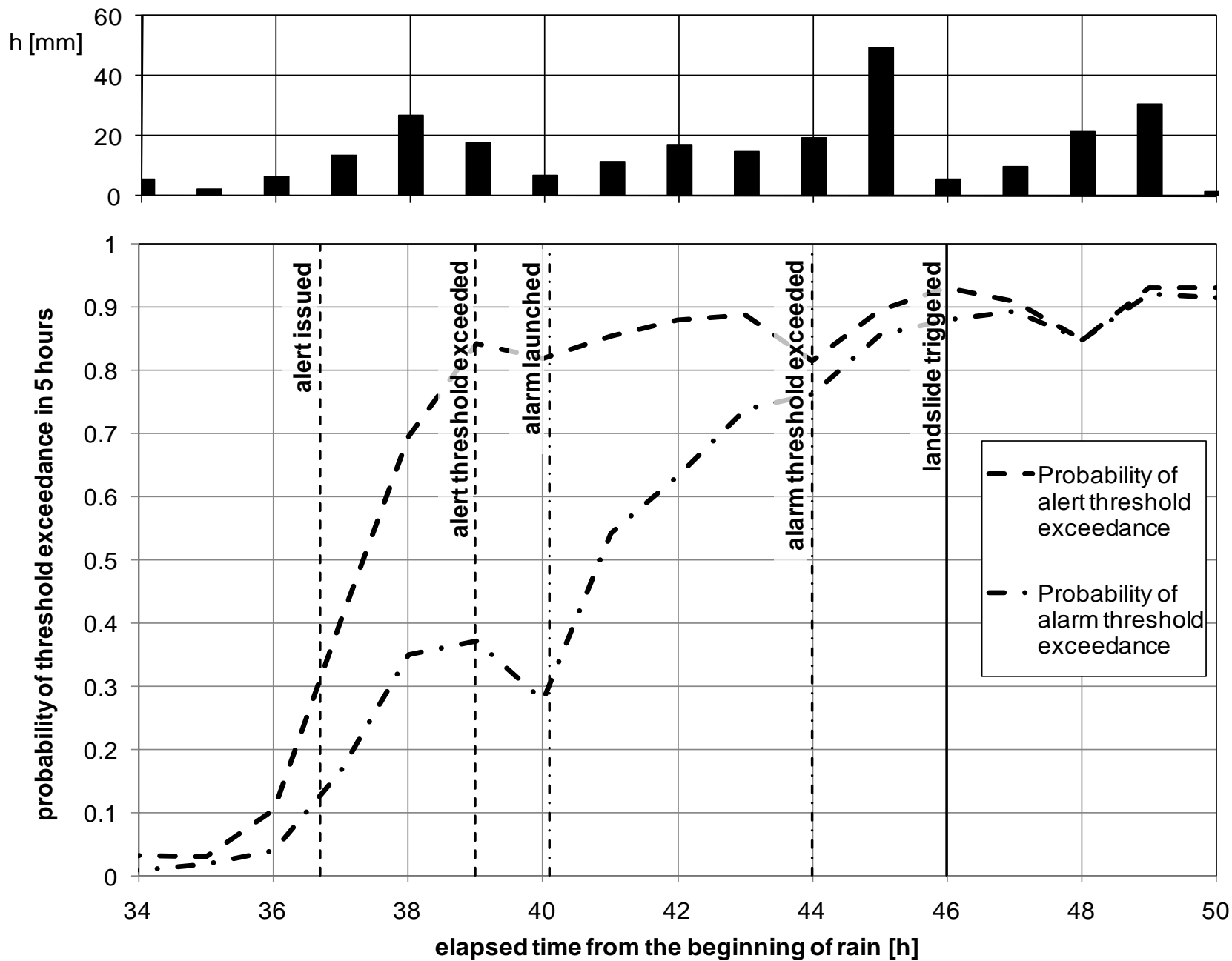


Figure 5



Figure 6

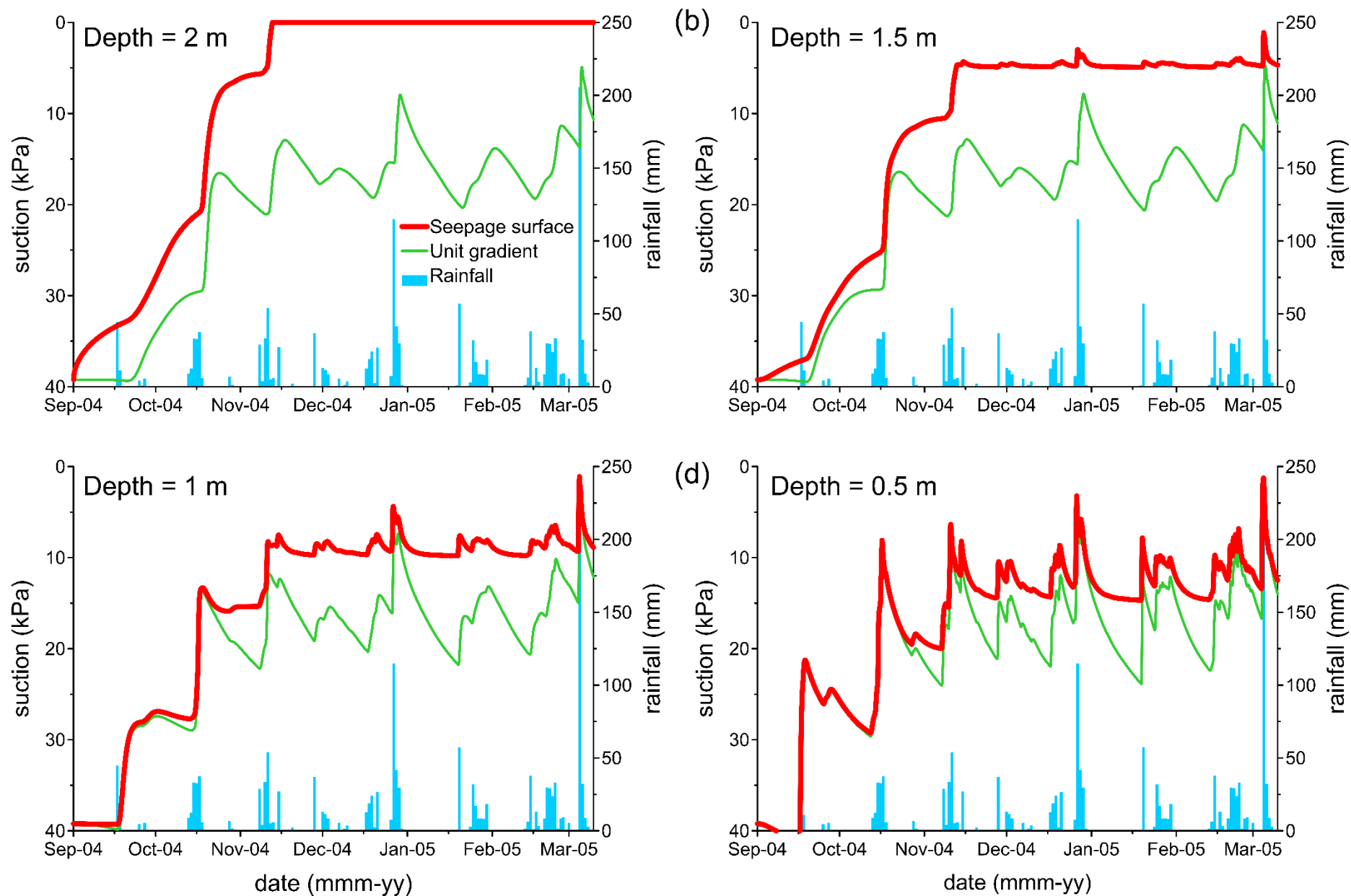


Figure 7